Endoplasmic Reticulum Stress Gene Induction and Protection From Ischemia/Reperfusion Injury in the Hearts of Transgenic Mice With a Tamoxifen-Regulated Form of ATF6

Joshua J. Martindale, Rayne Fernandez, Donna Thuerauf, Ross Whittaker, Natalie Gude, Mark A. Sussman and Christopher C. Glembotski

Circ. Res. 2006;98;1186-1193; originally published online Apr 6, 2006;
DOI: 10.1161/01.RES.0000220643.65941.8d
Circulation Research is published by the American Heart Association. 7272 Greenville Avenue, Dallas, TX 72514
 Print ISSN: 0009-7330. Online ISSN: 1524-4571

Endoplasmic Reticulum Stress Gene Induction and Protection From Ischemia/Reperfusion Injury in the Hearts of Transgenic Mice With a Tamoxifen-Regulated Form of ATF6

Joshua J. Martindale, Rayne Fernandez, Donna Thuerauf, Ross Whittaker, Natalie Gude, Mark A. Sussman, Christopher C. Glembotski

***Abstract*—**Ischemia/reperfusion (I/R) affects the integrity of the endoplasmic reticulum (ER), the site of synthesis and folding of numerous proteins. Therefore, I/R may activate the unfolded protein response (UPR), resulting in the induction of a collection of ER stress proteins, many of which are protective and function to resolve the ER stress. In this study, we showed that when mouse hearts were subjected to ex vivo I/R, the levels of 2 ER stress-inducible markers of the UPR, the ER-targeted cytoprotective chaperones glucose-regulated proteins 78 and 94 (GRP78 and GRP94), were increased, consistent with I/R-mediated UPR activation in the heart. The UPR-mediated activation of ATF6 (Activation of Transcription Factor 6) induces cytoprotective ER stress proteins, including GRP78 and GRP94. To examine whether ATF6 protects the myocardium from I/R injury in the heart, we generated transgenic (TG) mice featuring cardiac-restricted expression of a novel tamoxifen-activated form of ATF6, ATF6-MER. When NTG and ATF6-MER TG mice were treated with or without tamoxifen for 5 days, only the hearts from the tamoxifen-treated TG mice exhibited increased levels of many ER stress–inducible mRNAs and proteins; for example, GRP78 and GRP94 transcript levels were increased by 8- and 15-fold, respectively. The tamoxifen-treated TG mouse hearts also exhibited better functional recovery from ex vivo I/R, as well as significantly reduced necrosis and apoptosis. These results suggest that the UPR is activated in the heart during I/R and that, as a result, the ATF6 branch of the UPR may induce expression of proteins that can function to reduce I/R injury. **(*Circ Res*. 2006;98:1186-1193.)**

Key Words: unfolded protein response ■ ischemia/reperfusion ■ ATF6

Ischemia and reperfusion (I/R) injury causes a loss of cardiac function via oxidative stress, calcium dysregulation, and eventual myocyte death.[1] The endoplasmic reticulum (ER) senses oxidative stress, maintains calcium homeostasis, and can trigger apoptotic signaling.[2,3] I/R can affect the ability of the ER to synthesize, fold, and sort proteins and may, therefore, lead to ER stress and activation of the unfolded protein response (UPR). The UPR alleviates ER stress by decreasing protein synthesis and increasing the expression of molecular chaperones that promote proper folding[4] and cellular recovery. However, if the ER stress goes unresolved, the UPR can initiate apoptosis.[5] Recent reports show that the UPR is activated in cardiac myocytes in response to hypoxia[6] and may play a role in the pathogenesis of heart disease.[7]

An important mediator of ER stress is ATF6 (Activation of Transcription Factor 6), a 670 amino acid ER-transmembrane protein with the N terminus oriented toward the cytosol and the C terminus toward the ER lumen.[8] ER stress causes the translocation of ATF6 from the ER to the Golgi,[9] where it is cleaved by regulated intramembrane proteolysis (RIP).[10] The resulting N-terminal portion of ATF6, approximately 400 amino acids, translocates to the nucleus, where it induces expression of numerous proteins involved with reestablishing ER homeostasis.[8] The role of the UPR in I/R damage has been studied to some extent in the brain[11–13] and in tumor cells[14,15]; however, only a few studies have touched on the role of the UPR in the heart. The UPR is active in the myocardium following transaortic constriction,[16] suggesting a role for the UPR during myocardial overload. Also, a mutant form of the KDEL receptor, which is involved with ER protein targeting, induced the UPR in the heart and caused dilated cardiomyopathy.[7] We recently showed that ATF6 is activated in cardiac myocytes by ER stress.[17] Several ATF6-inducible gene products protect cardiac myocytes and/or the heart from various stresses, including I/R.[18,19] In the present study, we determined whether activated ATF6 protects the myocardium from I/R injury. We developed a novel ligand-

Original received October 26, 2005; revision received February 27, 2006; accepted March 27, 2006.

From the San Diego State University Heart Institute and Department of Biology, San Diego State University, Calif.

Correspondence to Christopher C. Glembotski, SDSU Heart Institute and Department of Biology, San Diego State University, San Diego, CA 92182. E-mail cglembotski@sciences.sdsu.edu

Circulation Research **is available at http://circres.ahajournals.org** **DOI: 10.1161/01.RES.0000220643.65941.8d**

regulated form of ATF6 by fusing a constitutively active N-terminal fragment of ATF6 to the mutated estradiol receptor (MER). Transgenic (TG) mice that express this ATF6-MER fusion protein in cardiac myocytes were prepared; although the ATF6-MER fusion protein was constitutively expressed in mouse heart myocytes, it was active only in the presence of tamoxifen. The hearts of ATF6-MER TG mice exhibited tamoxifen-dependent protection from I/R-induced injury, as well as the induction of numerous ER stress response genes that encode potentially protective proteins.

Materials and Methods

Primary Neonatal Rat Cardiomyocyte Cultures

Primary cultures of neonatal rat ventricular cardiomyocytes (NRVCMs) were prepared as previously described.[20]

Luciferase Assays

NRVCMs were cotransfected with plasmids encoding SV40–β-galactosidase (pCH110, Amersham), glucose-regulated protein 78 (GRP78)-ERSE-luc, and ATF6(39-373)-MER. After 24 hours in 10% FBS, cells were treated with vehicle (ethanol) or tamoxifen for 24 hours. Cells were harvested for reporter enzyme assays as previously described.[21]

Animals

Approximately 300 C57/BL6 mice (Harlan Sprague–Dawley), 8 to 12 weeks old were studied. All procedures involving animals were in accordance with the San Diego State University Institutional Animal Care and Use Committee. Unless otherwise noted, each experiment was performed using a mixture of male and female mice.

Generation of ATF6-MER TG Mice

Constructs encoding various forms of Flag-ATF6 were prepared as described[21] and then fused to amino acids 281 to 599 of the murine estrogen receptor (ER) harboring a G-to-R mutation at amino acid 525, a gift from Michael Reth (Max-Plank Institute, Freiburg, Germany). The Flag-ATF6-MER cDNAs were cloned into the α-MHC vector, a gift from J. Robbins (University of Cincinnati). The α-MHC-Flag-ATF6-MER construct was linearized and injected into the pronuclei of fertilized B6D2F1 (Harlan Sprague–Dawley) embryos. The resulting TG mice were back-bred into the C57/BL6 background strain for at least 5 generations. Animals were genotyped by isolating DNA from tail biopsies and performing PCR with the following primers: ATF6-MER primers (5′ primer: CAGACGGTTTTGCTGTCTCAG; 3′ primer: ACCCATTTCATTTCGTAGCG); β-globin primers (5′ primer: CCAATCTGCTCACACAGGATAGAGAGGGCAGG; 3′ primer: CCTTGAGGCTGTCCAAGTGATTCAGGCCATCG).

Tamoxifen Treatments

Tamoxifen (Sigma, St Louis, Mo) was suspended at 10 mg/mL in 100 μL of 95% ethanol and 900 μL of sunflower oil and sonicated until clarified. Animals were injected IP with 20 mg/kg tamoxifen (Sigma) or vehicle (95% ethanol and sunflower oil only) daily for 5 days.

Tissue Extracts

Frozen mouse tissues were pulverized and sonicated in sodium dodecyl sulfate (SDS) lysis buffer (50 mmol/L Tris pH 7.5, 20 mmol/L β-glycerophosphate, 250 mmol/L NaCl, 2 mmol/L dithiothreitol, 1 mmol/L phenylmethylsulfonyl fluoride, 10 μg/mL leupeptin, 3 mmol/L EDTA, 3 mmol/L EGTA, 0.1 mmol/L Na orthovanadate, 1 mmol/L *p*-nitrophenyl phosphate, 10 μg/mL aprotinin, 0.5% SDS, 1 μL/mL benzonase [Calbiochem, San Diego, Calif]). Lysates were centrifuged at 14 000*g* for 10 minutes. Protein was determined using the DC Protein Assay Kit (Bio-Rad, Hercules, Calif).

Immunoblotting

Tissue extracts (25 to 50 μg of protein) were fractionated on Bio Criterion XT Precast Gels (Bio-Rad) and transferred to polyvinylidene difluoride membranes (Perkin Elmer, Boston, Mass). Primary antibodies used for immunoblotting were anti-Flag (Sigma); anti-KDEL, which cross-reacts with GRP94 and 78,[10,22,23] and anti-ERp72 (Stressgen, Victoria, BC); anti-ATF6 (N terminus), anti-GRP78, anti-CHOP/GADD153, anti-PDI (Santa Cruz Biotechnology, Santa Cruz, Calif); and anti-GAPDH (Research Diagnostics, Concord, Mass). Secondary antibodies were horseradish peroxidase–conjugated (Jackson Immunoresearch, West Grove, Pa). Membranes were incubated with ECL Plus (Amersham, Piscataway, NJ), and chemifluorescence was assessed on a Molecular Dynamics Storm System. Quantification was performed using ImageQuant v5.2.

RNA Analysis

RNA was extracted from hearts using RNAzol (Tel-Test, Friendswood, Tex). cDNA was generated by reverse transcriptase reaction using Superscript III (Invitrogen, Carlsbad, Calif). Real-time quantitative PCR was performed on cDNAs using the Quanti-Tect SYBR Green PCR Kit (Qiagen, Valencia, Calif) and an ABI Prism 7000 (Applied Biosystems, Foster City, Calif). The following primers were used:

1. ANP: 5′-GCTTCCAGGCCATATTGGAG; 3′-GGGGGCATGACCTCATCTT
2. Armet: 5′-AGAAGATCCTGGACGACTGGG; 3′-ACTTTTCTGCACAGCCTTTGC
3. β-Myosin heavy chain: 5′-AGATGTTTTTGTGCCCGATGA; 3′-CAGTCACCGTCTTGCCATTCT
4. Calnexin: 5′-GGGAGTCTTGTCGTGGAATTG; 3′-TGCTTTCCAAGACGGCAGA
5. Calreticulin: 5′-ACATCAGGAGCTAAAAGCA-GCC; 3′-TGAAACATACGTCACCCGCA
6. Chop: 5′-CATGAACAGTGGGCATCACC; 3′-GC-TGGGTACACTTCCGGAGAG
7. EDEM: 5′-GACCCACCGCTCTACGTCAA; 3′-GT-TCATGAGCTGCCCACTGA
8. ERdj4: 5′-CTTGTGCCTTTGGCCACTG; 3′-CAC-AGAGTGGCATGTCACCC
9. ERO-1L: 5′-AAGGGCTCTCTCCAAAGTGCT; 3′-AGCTGAAAATCTGGACGCTCA
10. ERp72: 5′-CCAGCTCTGCACCCAATCAT; 3′-CAGGACCAACAGCCAAGCTT
11. GAPDH: 5′-ATGTTCCAGTATGACTCCACTCACG; 3′-GAAGACACCAGTAGACTCCACGACA
12. GRP78: 5′-CACGTCCAACCCCGAGAA; 3′-AT-TCCAAGTGCGTCCGATG
13. GRP94: 5′-GGGAGGTCACCTTCAAGTCG; 3′-CTCGAGGTGCAGATGTGGG
14. Herp: 5′-CGTTCAGACAGAGGCCAGTTC; 3′-CT-CGAGGACCACCATCATCC
15. P5: 5′-GGAAGAAAGCAGCAACGGC; 3′-TGAC-GGCCCCGACTTTAAC
16. $p58^{IPK}$: 5′-CTTAAATCTGAACGGTCCGCC; 3′-GTTGGAACTCATGGCAAGGGT
17. PDI: 5′-TAGCAAAGGTGGATGCCACA; 3′-CAC-CATACTGCTGAGCCAGGT
18. PDIR: 5′-CTCAGGACCCGCAATAACGT; 3′-TG-CTACCTCGGATTCCGAGT
19. Xbp1: 5′-ACGGCCTTGTGGTTGAGAAC; 3′-TG-TCCATTCCCAAGCGTGTT

Relative abundance of RNA was calculated by the ΔΔCt method.[24] Primers were designed using Primer Express v2.0 (Applied Biosystems, Foster City, Calif). All primers were between 90% to 110% efficient, as assessed by standard curve, and all displayed only 1 dissociation peak.

Echocardiography

Mice were anesthetized with isofluorane, and transthoracic 2D guided M-mode echocardiography was performed using an Acuson Sequoia C256 echocardiograph as previously described.[25]

Global I/R

Hearts from age-matched (8 to 12 weeks of age) non-TG (NTG) and ATF6-MER TG mice treated with or without tamoxifen were exposed to global no-flow ischemia and reperfusion at 37°C at a flow rate of 2 to 4 mL/min and a pressure of 80 mm Hg, as previously described.[26]

Lactate Dehydrogenase Assays

Perfusates from the hearts subjected to global I/R were collected after 30 minutes of reperfusion. Aliquots (100 μL) of perfusate were added to an equal volume of lactate dehydrogenase (LDH) assay buffer (240 nmol/L NADH, 5 mmol/L pyruvate, 0.06% BSA in 100 mmol/L phosphate buffer [pH 7.5]). LDH units indicate change in absorbance [NADH] normalized to protein.

Triphenyl Tetrazolium Chloride Staining

Hearts exposed to global ischemia and reperfusion were frozen at −80°C. Hearts were partially thawed and sliced into 1-mm sections. Sections were incubated in 1% triphenyl tetrazolium chloride (TTC) in phosphate buffer (Na_2HPO_4 88 mmol/L, NaH_2PO_4 1.8 mmol/L) at 37°C for 10 minutes. Sections were placed on glass slides and scanned on a Canon scanner. Images were quantified using a Wacom tablet and pen with ImageJ to outline the infarct and area at risk.

Terminal Deoxynucleotidyltransferase-Mediated dUTP Nick End Labeling

Hearts exposed to I/R were fixed in 10% neutral-buffered formalin and embedded in paraffin, and 5-μm sections were prepared. Cardiac myocytes were stained with anti–sarcomeric actinin (1:200 dilution; Sigma) followed by goat anti-mouse fluorescein isothiocyanate (FITC) (1:200 dilution; Invitrogen). Nuclei were stained with TOPRO-3 (0.1 μg/mL; Invitrogen). Apoptotic nuclei were labeled using the *In Situ* Cell Death Detection Kit, TMR Red (Roche Applied Science, Indianapolis, Ind). The samples were examined by confocal microscopy using a Leica confocal microscope. Apoptotic nuclei shown to be surrounded by colocalizing actinin were scored as apoptotic cardiac myocytes.

Statistics

Data are reported as mean±SEM and analyzed via 1-way ANOVA with Newman–Keuls correction using SPSS version 11.0.

Results

Because I/R affects the integrity of the ER, we determined whether the UPR is activated in the myocardium in response to I/R. Accordingly, isolated perfused mouse hearts were treated with or without I/R, and tissue extracts were analyzed for the levels of glucose-regulated proteins 78 and 94 (GRP78, GRP94), which are well-characterized indicators of UPR activation.[27] Compared with control, extracts from hearts subjected to I/R for this brief time exhibited increased GRP94 and 78 (Figure 1A). Although it is unclear whether this induction is beneficial in this setting, these results are consistent with the possibility that ATF6 is activated by I/R.

Because UPR-mediated activation of the transcription factor ATF6 induces numerous cytoprotective proteins, we determined the effects of expressing activated ATF6 in TG mouse hearts. To obviate any effects of the transgene on postnatal cardiac development, we developed a version of ATF6 that could be activated by the estrogen analogue tamoxifen, as has been done for Cre recombinase and c-myc.[28,29] The MER was fused to either the N terminus or the C terminus or to both ends of constitutively active forms of ATF6, ie, those that do not possess an ER transmembrane domain but retain a transactivation and DNA-binding domain. When tested in cultured cells, the construct exhibiting the lowest basal activity and the greatest tamoxifen-inducible

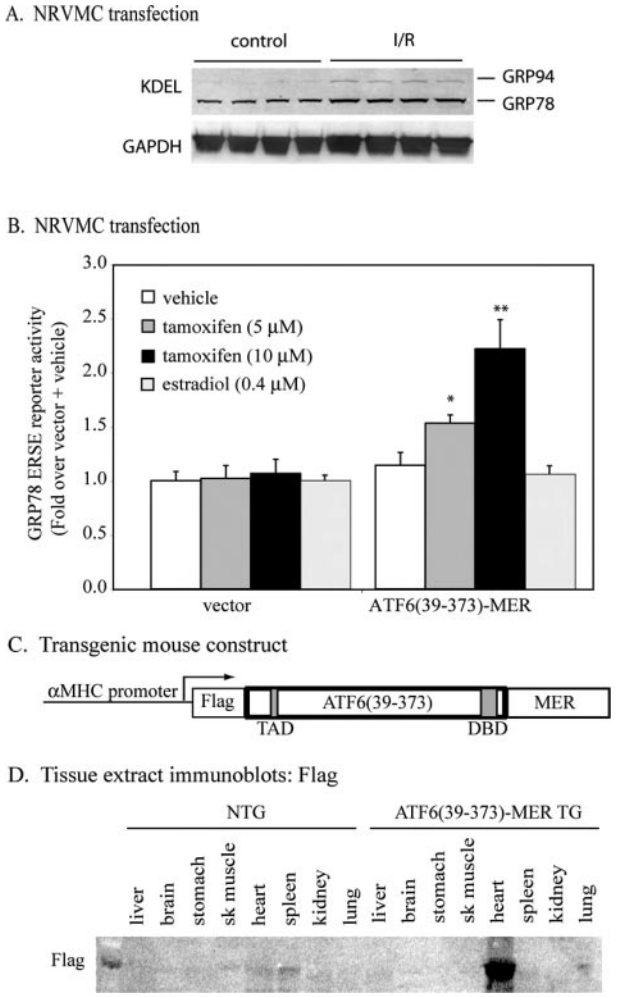

Figure 1. Ex vivo I/R of NTG mouse hearts, tamoxifen-regulated activation of Flag-ATF6-MER and generation of Flag-ATF6-MER TG mice. A, Hearts from C57/BL6 mice were equilibrated for 175 minutes and then extracted (control) or equilibrated for 30 minutes, followed by 25 minutes of global no-flow ischemia and then 2 hours of reperfusion (I/R) and then extracted. Extracts were fractionated by SDS-PAGE and immunoblotted with anti-GAPDH antibody or with anti-KDEL antibody, which detects the ER-targeting sequence KDEL in GRP78 and GRP94. B, Cardiac myocytes were cotransfected with plasmids encoding Flag-ATF6(39-373)-MER, GRP78-ERSE-luc, and SV40–β-galactosidase (pCH110). After 24 hours in 10% FBS, cells were treated with 5 or 10 μmol/L tamoxifen or with 0.2 μmol/L estradiol for 24 hours. Cultures were then extracted for reporter enzyme assays. Shown are the mean values for relative luciferase (luciferase/β-galactosidase) of triplicate cultures±SEM. $^{**}P<0.001$, $^{*}P<0.05$, different from all other values. C, Schematic diagram of α-MHC-Flag-ATF6(39-373)-MER cDNA used to generate TG mice. TAD indicates transcriptional activation domain located at AA 39 to 78[21]; DBD, DNA-binding domain. D, Immunoblotting of various tissue extracts from NTG and ATF6-MER TG mice using anti-Flag antibody. Fifty micrograms of protein were fractionated in each lane.

activity encodes ATF6(39-373) with MER fused to the C terminus, ie, ATF6(39-373)-MER (data not shown). Co-transfection of ATF6(39-373)-MER and GRP78-ERSE-luciferase, a well-characterized ATF6-inducible reporter,[17] showed that in the absence of tamoxifen, ATF6(39-373)-MER exhibited no apparent reporter activity relative to vector alone. In contrast, in the presence of 5 or 10 μmol/L tamoxifen, ATF6(39-373)-MER exhibited approximately 1.5-fold ($P<0.05$) or 2.5-fold ($P<0.001$) increases in reporter activity, respectively (Figure 1B). ATF6(39-373)-MER was not responsive to supraphysiological levels of estradiol (0.2 μmol/L). This finding is consistent with previous studies showing that the MER cannot bind estrogen.[29–31] In vehicle treated cultures, ATF6(39-373)-MER was found to reside primarily in the cytosol, whereas tamoxifen treatment increased localization to the nucleus (not shown).

The Flag-ATF6(39-373)-MER cDNA was cloned into the α-myosin heavy chain (α-MHC) promoter construct to create α-MHC-Flag-ATF6-Mer (Figure 1C), which was used to generate ATF6-MER TG mice. Flag immunoblotting demonstrated the cardiac specificity of transgene expression (Figure 1D). Several lines of ATF6-MER TG mice that exhibited somewhat different levels of transgene expression were generated (Figure 2A; Flag, lanes 1 to 6). In general, transgene expression was similar to the levels of endogenous ATF6 expression (Figure 2A; ATF6; **, transgene; *, endogenous; lanes 1 to 6). Whereas the levels of endogenous ATF6 did not change on treatment with tamoxifen (Figure 2A; ATF6, *, lanes 1 to 6 [vehicle] versus 9 to 16 [tamoxifen]), ATF6-MER levels were lower after tamoxifen treatment (Figure 2A; ATF6, **, lanes 1 to 6 [vehicle] versus 9 to 16 [tamoxifen]). This finding is consistent with our previous studies showing that ATF6 becomes more labile when activated[21] and provides further evidence that tamoxifen facilitates the activation of ATF6-MER but not endogenous ATF6, as desired. To assess the ability of ATF6-MER to confer gene induction in vivo, we examined the levels of several known ATF6-inducible proteins. The levels of GRP78 and GRP94 were highest in hearts from tamoxifen-treated ATF-MER TG mice (Figure 2B; GRP78 and KDEL; lanes 1 to 6 [vehicle] versus 9 to 16 [tamoxifen]), which was also observed for 2 other ATF6-inducible proteins, protein disulfide isomerase (PDI) and ERp72 (Figure 2C; PDI and ERp72). However, the proapoptotic protein CHOP which is also regulated by the UPR,[32] was not induced (Figure 2D; CHOP IB), suggesting ATF6 alone does not regulate CHOP protein expression. Mouse line 5644, which exhibited the highest level of ATF6-MER expression, was selected for further study.

The relative abundance of mRNAs encoding several UPR proteins was analyzed by real-time quantitative RT-PCR. The levels of GRP78 and GRP94 mRNA were increased by 8-fold ($P<0.05$) and 15-fold ($P<0.01$), respectively, but only in hearts from tamoxifen-treated ATF-MER TG mice (Figure 3A). Members of the PDI family showed similar results, where only the hearts from tamoxifen-treated ATF6-MER mice exhibited a 20-fold increase in PDI ($P<0.001$), with increases in the PDI homologs P5 and ERp72 of 5-fold ($P<0.01$) and 35-fold ($P<0.001$), respectively (Figure 3B). Herp, a protein involved with ER-associated degradation

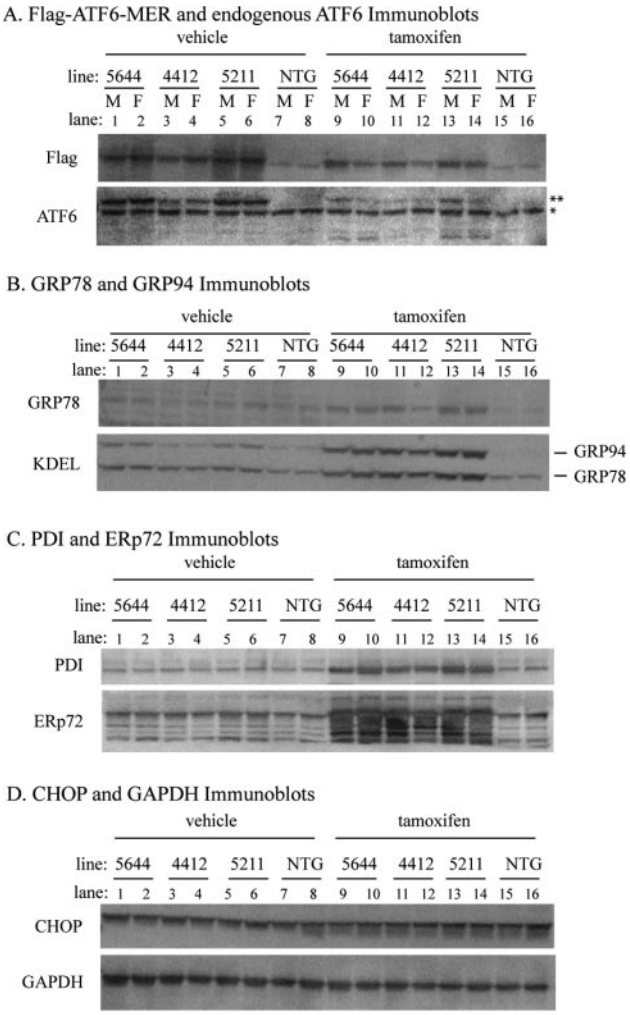

Figure 2. Immunoblotting of ER stress–related proteins in NTG and ATF6-MER TG mouse hearts. NTG mice and mice from several lines of ATF6-MER TG mice were treated with or without tamoxifen (20 mg/kg) by IP injection daily for 5 days. Aliquots of 25 to 50 μg of cardiac extract protein were assessed by immunoblotting. A, Cardiac extracts from NTG mice and ATF6-MER TG mice from lines 5644, 4412, and 5211 (M, male; F, female) treated with or without tamoxifen were immunoblotted for the transgene (Flag) or endogenous ATF6. Endogenous ATF6 is indicated by *, and the TG ATF6-MER fusion protein is indicated by **. B, Cardiac extracts from animals, as described in Figure 2A, were immunoblotted with a GRP78-specific antibody or with a KDEL-antibody, which detects both GRP78 and GRP94. C and D, Cardiac extracts were immunoblotted for the protein disulfide isomerases PDI and ERp72 (C) or for the proapoptotic protein CHOP (D). GAPDH was used as the loading control for all immunoblots.

(ERAD) of misfolded proteins, showed a 15-fold tamoxifen-dependent increase in only the ATF6-MER TG mouse hearts ($P<0.002$) (Figure 3C). The mRNA levels of EDEM, which is also involved in ERAD, showed an apparent increase in hearts from tamoxifen-treated ATF6-MER TG mice, but this change did not reach significance (Figure 3C). The mRNA levels of other genes involved with the UPR (namely XBP1, p58^{ipk}, and CHOP) showed apparent increases in tamoxifen-treated ATF6-MER TG mouse hearts, but none of these changes reached statistical significance (Figure 3D). SERCA-2, a gene we previously characterized as ATF6

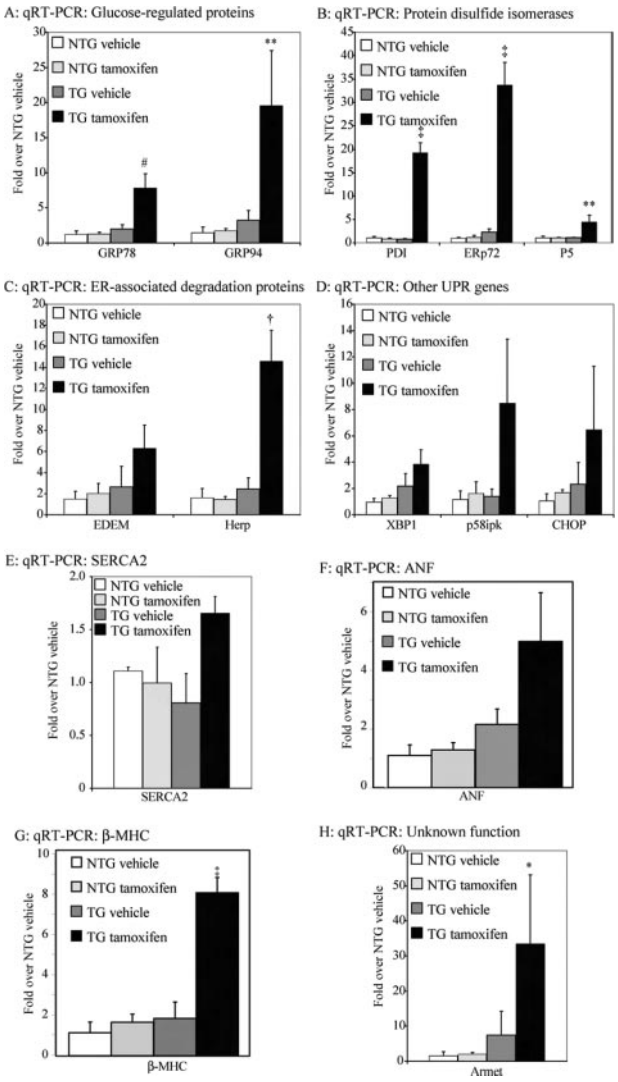

Figure 3. Quantification of ER stress–related mRNAs in NTG and ATF6-MER TG mouse hearts. NTG or ATF6-MER TG mice (female) were treated with or without tamoxifen, as in Figure 2. Real-time quantitative PCR (qRT-PCR) was performed on cDNAs, as described in the Materials and Methods. n=3 for each treatment group. ‡$P<0.001$, †$P<0.002$, **$P<0.01$, *$P<0.02$, #$P<0.05$ vs all other groups.

inducible, increased on tamoxifen treatment, but this change did not reach statistical significance (Figure 3E). A marker of cardiac hypertrophy, atrial natriuretic peptide, showed an approximate 5-fold increase, in only tamoxifen-treated TG mouse hearts, but it did not reach significance, and β-MHC showed an approximate 8-fold increase, which did reach significance (Figure 3F and 3G). The impact of this finding is unclear, because the tamoxifen-treated ATF6-MER mouse hearts showed no morphological or functional signs of hypertrophy (see below). Interestingly, mRNA levels for a gene of unknown function, Armet, which was previously shown to be induced during the UPR,[33] was increased >30-fold in only the hearts from tamoxifen-treated ATF6-MER TG mice (Figure 3H). Messenger RNA levels for the ER calcium-binding proteins, calnexin and calreticulin, the GRP78 ATPase, ERdj4, and the PDI oxidase, ERO-1L, were also assayed but showed no increase in ATF6-MER TG mice (data not shown).

Histology and echocardiography were performed to examine the effects of ATF6 on cardiac morphology and function. The histology indicated that the TG mice treated with or without tamoxifen exhibited no different cardiac morphological features than NTG mice (not shown). Echocardiography also showed that cardiac chamber sizes and wall thickness of all groups were essentially identical (Table), indicating that none of the treatments affected cardiac dimensions or function.

Because potentially protective proteins were upregulated in the hearts of tamoxifen-treated ATF6-MER mice, we determined whether the hearts would exhibit protection from the effects of ex vivo I/R. The hearts from female or male NTG mice treated with or without tamoxifen and ATF6-MER TG mice treated without tamoxifen showed a maximum left ventricle developed pressure (LVDP) recovery of approximately 20% to 40%, relative to equilibration at 30 minutes of reperfusion (Figure 4). In contrast, hearts from tamoxifen-treated male or female ATF6-MER TG mice exhibited an approximate 70% recovery of LVDP at 30 minutes of reperfusion, which remained statistically significant through 2 hours of reperfusion.

The release of LDH from isolated perfused mouse hearts was examined to assess necrosis. Only the perfusates from tamoxifen-treated ATF6-MER TG mouse hearts showed a significant decrease in LDH following I/R ($P<0.05$) (Figure 5A), indicating reduced necrosis. Hearts exposed to I/R were stained with TTC. Representative TTC stains display large areas of dead tissue (yellow) in hearts from NTG mice treated with or without tamoxifen and untreated ATF6-MER mice. Conversely, hearts from tamoxifen-treated ATF6-MER TG mice retained substantial viable tissue (red) (Figure 5B),

Echocardiographic Analysis of the Left Ventricle

	NTG		ATF6-MER TG	
	Vehicle	Tamoxifen	Vehicle	Tamoxifen
n	3	3	3	4
Heart rate, bpm	549±4	531±24	491±54	508±3
Anterior wall thickness, mm	0.76±0.02	0.82±0.05	0.79±0.04	0.75±0.04
Posterior wall thickness, mm	0.76±0.02	0.75±0.03	0.72±0.08	0.76±0.01
End-diastolic dimension, mm	3.15±0.13	3.48±0.21	3.58±0.41	3.54±0.12
End-systolic dimension, mm	2.01±0.05	2.24±0.16	2.33±0.52	2.44±0.08
Fractional shortening, %	35.8±3.9	35.5±2.1	35.9±6.9	31±1.8

Results are shown as mean±SEM.

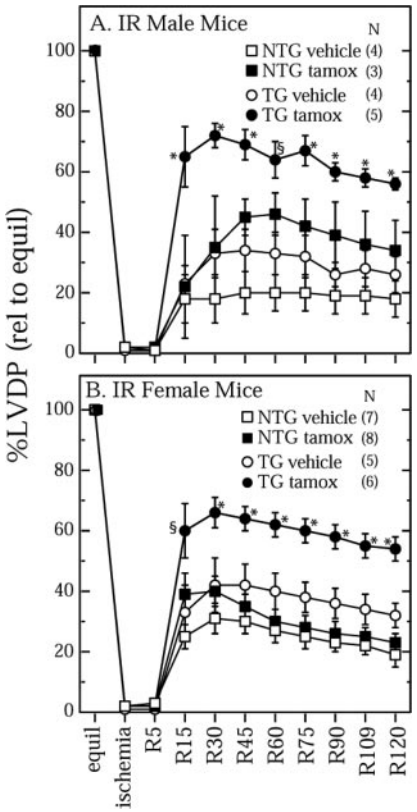

Figure 4. Ex vivo I/R of NTG and ATF6-MER TG mouse hearts. Hearts from male (A) or female (B) NTG and ATF6-MER TG mice treated with or without tamoxifen were equilibrated for 30 minutes, followed by 25 minutes of global no-flow ischemia and then 2 hours of reperfusion (I/R). LVDP was normalized to the pressure obtained during the equilibration (equil) period and set at 100%. *$P<0.05$ vs all other groups.

supporting the hypothesis that activated ATF6 protected the myocardium from I/R injury (Figure 5C).

To assess apoptosis, NTG and TG mice were treated with or without tamoxifen, hearts were isolated and subjected to ex vivo I/R and sectioned, and TUNEL staining was performed. Sections were labeled for sarcomeric actinin to identify cardiac myocytes (Figure 6A), with TOPRO-3 to label nuclei (Figure 6B), and with TUNEL reactions to identify apoptotic cells (Figure 6C). Only TUNEL-positive cells that were clearly surrounded by sarcomeric actinin were scored as apoptotic cardiac myocytes (Figure 6D, arrow). Hearts from NTG mice treated with or without tamoxifen, as well as untreated ATF6-MER TG mice exposed to I/R, exhibited approximately 8% to 10% TUNEL-positive cardiac myocytes in the left ventricle; however, the hearts from tamoxifen-treated ATF6-MER TG mice exhibited only 3% TUNEL-positive cardiac myocytes ($P<0.05$) (Figure 6E). Taken together with results in Figure 5, these findings are consistent with the hypothesis that activated ATF6 decreased I/R-mediated myocardial tissue damage, necrosis, and apoptosis.

Discussion

The data presented here support the hypothesis that the UPR is induced by I/R in the myocardium, and that the ATF6 branch of the UPR may contribute to protecting the myocardium from I/R damage. Acute activation of ATF6 increased the expression of several ATF6-inducible proteins. This pre-induction of potentially protective proteins may have been responsible for reduced myocardial I/R damage, decreased necrosis and apoptosis, and it may have fostered better functional recovery from I/R, as shown by increased LVDP. To our knowledge, this is the first study to report the protective effects of ATF6 in any tissue, in vivo, and the first demonstration of ATF6-mediated protection of the myocardium from I/R injury.

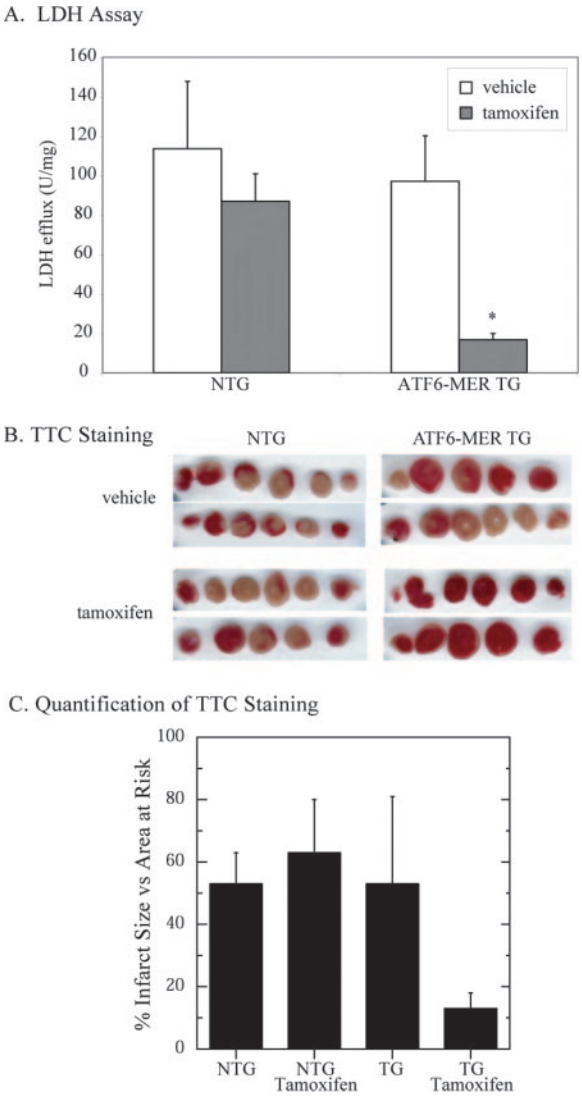

Figure 5. I/R-induced damage in NTG and ATF6-MER TG mouse hearts. A, After 30 minutes of equilibration, hearts were exposed to 25 minutes of ischemia followed by 30 minutes of reperfusion. Samples of perfusate were obtained at 30 minutes of reperfusion to assess LDH levels. *$P<0.05$ vs all other groups; n=3. B, Hearts were exposed to 25 minutes of ischemia and 2 hours of reperfusion, and sections were stained with TTC to qualitatively assess the extent of myocardial infarction. Tissue stained positive appears red and represents viable myocardium. Myocardium that does not stain positive appears yellow and represents infarcted tissue. C, TTC-stained heart sections shown in B were quantified as described in Materials and Methods, and shown is the average infarct size vs area at risk±SD (n=2 TG and 2 NTG hearts per treatment).

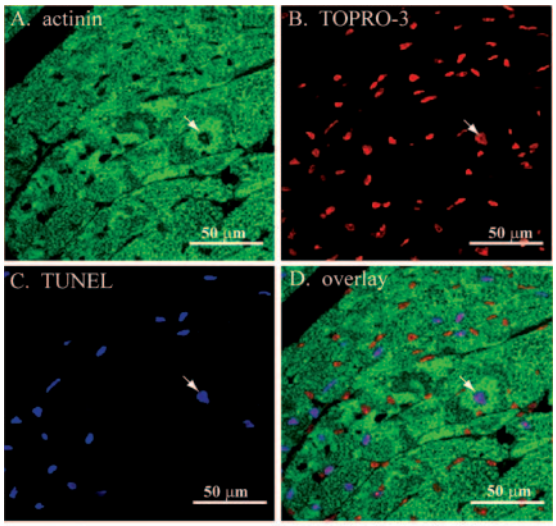

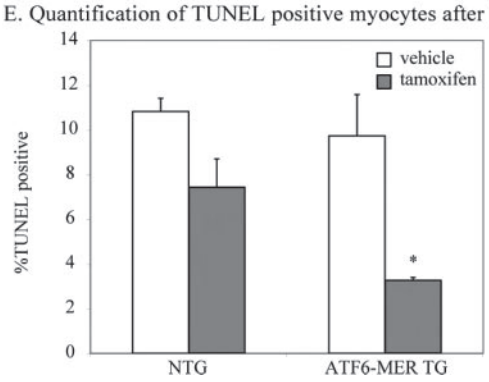

Figure 6. TUNEL analysis of NTG and ATF6-MER TG mouse hearts following I/R. Hearts were exposed to I/R as described in Figure 4 and Materials and Methods. Representative confocal microscope images depicting staining for sarcomeric actinin (A), TOPRO-3 (nuclei) (B), TUNEL (C), and an overlay (D) are shown. Arrows indicate an example of a TUNEL-positive myocyte. Three mouse hearts were used in each group, and 1500 to 3100 cells were counted in each group. The percentage of cells that exhibited TUNEL-positive nuclei surrounded by cardiac actinin (TUNEL-positive cardiac myocytes) are shown in E. *$P<0.05$ different from all other groups.

Previous studies support the hypothesis that certain ER stress inducible proteins may be protective in the heart. For example, overexpression of GRP94 in cardiac myocytes prevented hypoxia-induced cell death[19] and pre-induction of GRP78 protected cardiac myocytes from oxidative damage.[34] Moreover, endothelin-1-mediated protection from hypoxia in cardiac myocytes was ablated by an GRP78 antisense oligodeoxynucleotide.[18] Studies in other cell types also support hypothetical protective roles of some ER stress inducible proteins. For instance, overexpression of GRP94 in neuroblastoma cells protected them from hypoxia induced apoptosis, and expression of GRP94 anti-sense increased apoptosis.[35] Transfection of PDI into the hippocampus decreased ischemia-induced apoptosis and necrosis in this region of the brain[36] and overexpression of Herp in neural cells protected from ER stress–induced apoptosis.[37] Furthermore, the global deletion of $p58^{IPK}$ increased apoptosis of pancreatic β cells.[38]

Although the precise mechanisms by which ER stress–response proteins protect the heart from I/R damage remain to be determined, it is probable that this protection is achieved via the known effects of these proteins in other tissue and cell types. The ER chaperone activities of GRP78, GRP94, and perhaps ERp72 and PDI may be important for protection; however, GRP78, GRP94, Herp, and ERp72 are also ER calcium-binding proteins,[37,39] which help to maintain calcium homeostasis in the ER. PDI does not appear to bind calcium directly, but calcium affects its interaction with calreticulin, which in turn regulates the chaperone activity of PDI.[37,39] Thus, protection of the myocardium from I/R damage by ER stress–response proteins may be the combinatorial result of several mechanisms.

Like many other stress-signaling pathways, the UPR can exert both protective and damaging affects. It is believed that most of the initial UPR responses are oriented toward protection and resolution of the ER stress.[3] However, if the ER stress continues unresolved, the UPR pathways that are activated can enhance apoptosis, which may serve a surveillance role in removing cells that are irreversibly damaged by prolonged ER stress. In the ATF6-MER TG mouse model described in this study, the tamoxifen-mediated ATF6 activation and protection from ER stress may be mimicking the initial, protective role of the endogenous ER stress response. It is possible, however, that prolonged activation of the ATF6 branch of the UPR might have detrimental affects in the heart. Such UPR-mediated apoptosis occurs via several mechanisms, 1 of which involves ATF6-mediated induction of the proapoptotic transcription factor CHOP/GADD153.[40] Although we observed a small increase in CHOP mRNA in tamoxifen-treated ATF6-MER TG mouse hearts, CHOP protein levels did not appear to be induced. Perhaps posttranscriptional mechanisms are also required to induce expression of CHOP protein.[41]

The findings of this study have potential widespread implications beyond the myocardium, because the UPR is conserved among all eukaryotic cells and because the UPR has been suggested to participate in the progression of Alzheimer's disease, diabetes, and tumorigenesis. Future studies relating the time of ATF6 activation to the extent of myocardial protection, as well as studies examining the roles of other branches of the UPR during I/R damage, will further illuminate the potential involvement of ER stress in cardiac health and pathology.

Acknowledgments

This work was supported by NIH grants HL-63975, NS/HL-25037, and HL-75573 (to C.C.G). J.J.M was a Predoctoral Fellow of the American Heart Association. N.G. and R.W. were fellows of the Rees-Stealy Research foundation and the San Diego State University Heart Institute.

References

1. Scarabelli TM, Gottlieb RA. Functional and clinical repercussions of myocyte apoptosis in the multifaceted damage by ischemia/reperfusion injury: old and new concepts after 10 years of contributions. *Cell Death Differ.* 2004;11(suppl 2):S144–S152.
2. Szabadkai G, Rizzuto R. Participation of endoplasmic reticulum and mitochondrial calcium handling in apoptosis: more than just neighborhood? *FEBS Lett.* 2004;567:111–115.
3. Xu C, Bailly-Maitre B, Reed JC. Endoplasmic reticulum stress: cell life and death decisions. *J Clin Invest.* 2005;115:2656–2664.

4. Kaufman RJ. Orchestrating the unfolded protein response in health and disease. *J Clin Invest*. 2002;110:1389–1398.
5. Szegezdi E, Fitzgerald U, Samali A. Caspase-12 and ER-stress-mediated apoptosis: the story so far. *Ann N Y Acad Sci*. 2003;1010:186–194.
6. Terai K, Hiramoto Y, Masaki M, Sugiyama S, Kuroda T, Hori M, Kawase I, Hirota H. AMP-activated protein kinase protects cardiomyocytes against hypoxic injury through attenuation of endoplasmic reticulum stress. *Mol Cell Biol*. 2005;25:9554–9575.
7. Hamada H, Suzuki M, Yuasa S, Mimura N, Shinozuka N, Takada Y, Nishino T, Nakaya H, Koseki H, Aoe T. Dilated cardiomyopathy caused by aberrant endoplasmic reticulum quality control in mutant KDEL receptor transgenic mice. *Mol Cell Biol*. 2004;24:8007–8017.
8. Haze K, Yoshida H, Yanagi H, Yura T, Mori K. Mammalian transcription factor ATF6 is synthesized as a transmembrane protein and activated by proteolysis in response to endoplasmic reticulum stress. *Mol Biol Cell*. 1999;10:3787–3799.
9. Chen X, Shen J, Prywes R. The luminal domain of ATF6 senses endoplasmic reticulum (ER) stress and causes translocation of ATF6 from the ER to the Golgi. *J Biol Chem*. 2002;277:13045–13052.
10. Ye J, Rawson RB, Komuro R, Chen X, Dave UP, Prywes R, Brown MS, Goldstein JL. ER stress induces cleavage of membrane-bound ATF6 by the same proteases that process SREBPs. *Mol Cell*. 2000;6:1355–1364.
11. Paschen W, Yatsiv I, Shoham S, Shohami E. Brain trauma induces X-box protein 1 processing indicative of activation of the endoplasmic reticulum unfolded protein response. *J Neurochem*. 2004;88:983–992.
12. Paschen W, Aufenberg C, Hotop S, Mengesdorf T. Transient cerebral ischemia activates processing of xbp1 messenger RNA indicative of endoplasmic reticulum stress. *J Cereb Blood Flow Metab*. 2003;23:449–461.
13. DeGracia DJ, Montie HL. Cerebral ischemia and the unfolded protein response. *J Neurochem*. 2004;91:1–8.
14. Koumenis C, Naczki C, Koritzinsky M, Rastani S, Diehl A, Sonenberg N, Koromilas A, Wouters BG. Regulation of protein synthesis by hypoxia via activation of the endoplasmic reticulum kinase PERK and phosphorylation of the translation initiation factor eIF2alpha. *Mol Cell Biol*. 2002;22:7405–7416.
15. Blais JD, Filipenko V, Bi M, Harding HP, Ron D, Koumenis C, Wouters BG, Bell JC. Activating transcription factor 4 is translationally regulated by hypoxic stress. *Mol Cell Biol*. 2004;24:7469–7482.
16. Okada K, Minamino T, Tsukamoto Y, Liao Y, Tsukamoto O, Takashima S, Hirata A, Fujita M, Nagamachi Y, Nakatani T, Yutani C, Ozawa K, Ogawa S, Tomoike H, Hori M, Kitakaze M. Prolonged endoplasmic reticulum stress in hypertrophic and failing heart after aortic constriction: possible contribution of endoplasmic reticulum stress to cardiac myocyte apoptosis. *Circulation*. 2004;110:705–712.
17. Thuerauf DJ, Hoover H, Meller J, Hernandez J, Su L, Andrews C, Dillmann WH, McDonough PM, Glembotski CC. Sarco/endoplasmic reticulum calcium ATPase-2 expression is regulated by ATF6 during the endoplasmic reticulum stress response: intracellular signaling of calcium stress in a cardiac myocyte model system. *J Biol Chem*. 2001;276:48309–48317.
18. Pan YX, Lin L, Ren AJ, Pan XJ, Chen H, Tang CS, Yuan WJ. HSP70 and GRP78 induced by endothelin-1 pretreatment enhance tolerance to hypoxia in cultured neonatal rat cardiomyocytes. *J Cardiovasc Pharmacol*. 2004;44:S117–S120.
19. Vitadello M, Penzo D, Petronilli V, Michieli G, Gomirato S, Menabo R, Di Lisa F, Gorza L. Overexpression of the stress protein Grp94 reduces cardiomyocyte necrosis due to calcium overload and simulated ischemia. *FASEB J*. 2003;17:923–925.
20. Hoover HE, Thuerauf DJ, Martindale JJ, Glembotski CC. alpha B-crystallin gene induction and phosphorylation by MKK6-activated p38. A potential role for alpha B-crystallin as a target of the p38 branch of the cardiac stress response. *J Biol Chem*. 2000;275:23825–23833.
21. Thuerauf DJ, Morrison LE, Hoover H, Glembotski CC. Coordination of ATF6-mediated transcription and ATF6 degradation by a domain that is shared with the viral transcription factor, VP16. *J Biol Chem*. 2002;277:20734–20739.
22. Broquet AH, Thomas G, Masliah J, Trugnan G, Bachelet M. Expression of the molecular chaperone Hsp70 in detergent-resistant microdomains correlates with its membrane delivery and release. *J Biol Chem*. 2003;278:21601–21606.
23. Reddy RK, Mao C, Baumeister P, Austin RC, Kaufman RJ, Lee AS. Endoplasmic reticulum chaperone protein GRP78 protects cells from apoptosis induced by topoisomerase inhibitors: role of ATP binding site in suppression of caspase-7 activation. *J Biol Chem*. 2003;278:20915–20924.
24. Livak KJ, Schmittgen TD. Analysis of relative gene expression data using real-time quantitative PCR and the 2(-Delta Delta C(T)) method. *Methods*. 2001;25:402–408.
25. Tsujita Y, Kato T, Sussman MA. Evaluation of left ventricular function in cardiomyopathic mice by tissue Doppler and color M-mode Doppler echocardiography. *Echocardiography*. 2005;22:245–253.
26. Martindale JJ, Wall JA, Martinez-Longoria DM, Aryal P, Rockman HA, Guo Y, Bolli R, Glembotski CC. Over-expression of MKK6 in the heart improves functional recovery from ischemia in vitro and protects against myocardial infarction in vivo. *J Biol Chem*. 2005;280:669–676.
27. Lee AS. The ER chaperone and signaling regulator GRP78/BiP as a monitor of endoplasmic reticulum stress. *Methods*. 2005;35:373–381.
28. Petrich BG, Molkentin JD, Wang Y. Temporal activation of c-Jun N-terminal kinase in adult transgenic heart via cre-loxP-mediated DNA recombination. *FASEB J*. 2003;17:749–751.
29. Xiao G, Mao S, Baumgarten G, Serrano J, Jordan MC, Roos KP, Fishbein MC, MacLellan WR. Inducible activation of c-Myc in adult myocardium in vivo provokes cardiac myocyte hypertrophy and reactivation of DNA synthesis. *Circ Res*. 2001;89:1122–1129.
30. Littlewood TD, Hancock DC, Danielian PS, Parker MG, Evan GI. A modified oestrogen receptor ligand-binding domain as an improved switch for the regulation of heterologous proteins. *Nucleic Acids Res*. 1995;23:1686–1690.
31. Sohal DS, Nghiem M, Crackower MA, Witt SA, Kimball TR, Tymitz KM, Penninger JM, Molkentin JD. Temporally regulated and tissue-specific gene manipulations in the adult and embryonic heart using a tamoxifen-inducible Cre protein. *Circ Res*. 2001;89:20–25.
32. Ma Y, Brewer JW, Diehl JA, Hendershot LM. Two distinct stress signaling pathways converge upon the CHOP promoter during the mammalian unfolded protein response. *J Mol Biol*. 2002;318:1351–1365.
33. Lee AH, Iwakoshi NN, Glimcher LH. XBP-1 regulates a subset of endoplasmic reticulum resident chaperone genes in the unfolded protein response. *Mol Cell Biol*. 2003;23:7448–7459.
34. Zhang PL, Lun M, Teng J, Huang J, Blasick TM, Yin L, Herrera GA, Cheung JY. Preinduced molecular chaperones in the endoplasmic reticulum protect cardiomyocytes from lethal injury. *Ann Clin Lab Sci*. 2004;34:449–457.
35. Bando Y, Katayama T, Kasai K, Taniguchi M, Tamatani M, Tohyama M. GRP94 (94 kDa glucose-regulated protein) suppresses ischemic neuronal cell death against ischemia/reperfusion injury. *Eur J Neurosci*. 2003;18:829–840.
36. Tanaka S, Uehara T, Nomura Y. Up-regulation of protein-disulfide isomerase in response to hypoxia/brain ischemia and its protective effect against apoptotic cell death. *J Biol Chem*. 2000;275:10388–10393.
37. Chan SL, Fu W, Zhang P, Cheng A, Lee J, Kokame K, Mattson MP. Herp stabilizes neuronal Ca2+ homeostasis and mitochondrial function during endoplasmic reticulum stress. *J Biol Chem*. 2004;279:28733–28743.
38. Ladiges WC, Knoblaugh SE, Morton JF, Korth MJ, Sopher BL, Baskin CR, MacAuley A, Goodman AG, LeBoeuf RC, Katze MG. Pancreatic beta-cell failure and diabetes in mice with a deletion mutation of the endoplasmic reticulum molecular chaperone gene P58IPK. *Diabetes*. 2005;54:1074–1081.
39. Lee AS. The glucose-regulated proteins: stress induction and clinical applications. *Trends Biochem Sci*. 2001;26:504–510.
40. Okada T, Yoshida H, Akazawa R, Negishi M, Mori K. Distinct roles of activating transcription factor 6 (ATF6) and double-stranded RNA-activated protein kinase-like endoplasmic reticulum kinase (PERK) in transcription during the mammalian unfolded protein response. *Biochem J*. 2002;366:585–594.
41. Oyadomari S, Mori M. Roles of CHOP/GADD153 in endoplasmic reticulum stress. *Cell Death Differ*. 2004;11:381–389.